Published in final edited form as:
J Comp Neurol. 2010 August 1; 518(15): 3046–3064. doi:10.1002/cne.22379.

AGE CHANGES IN MYELINATED NERVE FIBERS OF THE CINGULATE BUNDLE AND CORPUS CALLOSUM IN THE RHESUS MONKEY

Michael P. Bowley[1,2], **Howard Cabral**[3], **Douglas L. Rosene**[1,4], and **Alan Peters**[1,4]

[1]Department of Anatomy and Neurobiology, Boston University School of Medicine, Boston, MA 02118

[2]Department of Medicine, Brigham and Women's Hospital, Boston, MA 02115

[3]Department of Biostatistics, Boston University School of Public Health, Boston, MA 02118

[4]Yerkes National Primate Research Center, Emory University, Atlanta, GA 30322

Abstract

Aging is accompanied by deficits in cognitive function, which may be related to the vulnerability of myelinated nerve fibers to the normal process of aging. Loss of nerve fibers, together with age-related alterations in myelin sheath structure, may result in the inefficient and poorly coordinated conduction of neuronal signals. Until now, the ultrastructural analysis of cerebral white matter fiber tracts associated with frontal lobe areas critical in cognitive processing has been limited. In this study we have analyzed the morphology and area number density of myelinated nerve fibers in the cingulate bundle and genu of the corpus callosum in behaviorally assessed young, middle aged, and old rhesus monkeys (*Macaca mulatta*). In both structures, normal aging results in a 20% decrease in the number of myelinated nerve fibers per unit area, while remaining nerve fibers exhibit an increasing frequency of degenerative changes in their myelin sheaths throughout middle and old age. Concomitantly, myelination continues in older monkeys, suggesting ongoing, albeit inadequate, reparative processes. Despite similar patterns of degeneration in both fiber tracts, only the age-related changes in the cingulate bundle correlate with declining cognitive function, underscoring its role as a critical corticocortical pathway linking the medial prefrontal, cingulate, and parahippocampal cortices in processes of working memory, recognition memory, and other higher cognitive faculties. These results further demonstrate the important role myelinated nerve fiber degeneration plays in the pathogenesis of age-related cognitive decline.

Keywords

Axon; Cingulum; Cognitive Decline; Paranode; Remyelination

INTRODUCTION

Aging in the cerebral white matter of primates is associated with degeneration of both the axons and sheaths of myelinated nerve fibers. Electron microscopic analyses in the rhesus monkey (*Macaca mulatta*) have shown that the normally compact myelin sheaths of some fibers develop degenerative alterations. These include a splitting of sheaths at the major dense line with an accumulation of dense cytoplasm (Peters et al., 2000; Sandell and Peters,

Correspondence to: Michael P. Bowley, M.D., Ph.D. Department of Anatomy and Neurobiology Boston University School of Medicine 700 Albany Street, W-701 Boston, MA, 02118 **Phone:** (617) 470-0810 **Fax:** (617) 638-4922 mpbowley@partners.org.

2001), as well as separations at the intraperiod line that result in balloon-like, fluid-filled, expansions of sheaths (Feldman and Peters, 1989). Simultaneously, other age-related changes in myelin sheaths suggest that myelination is continuing. For example, there is an increased frequency of myelinated nerve fiber profiles through paranodes, suggesting that the total number of internodal lengths of myelin increases in older monkeys (Peters and Sethares, 2003). There is also an increase in the percentage of profiles of myelin internodes with inappropriately thin sheaths (Peters and Sethares, 2003). Both thin sheaths and short internodal lengths of myelin are classic signs of remyelination in the central nervous system (Gledhill and McDonald, 1977; Ludwin, 1978; 1981; Hirano, 1989). Further indicators of continued myelination with age are the presence of some sheaths with large, redundant loops of myelin that extend away from their enclosed axon (Rosenbluth, 1966; Sturrock, 1976; Peters et al., 2000), as well as a significant increase in the average number of myelin lamellae encircling an individual axon (Peters et al., 2001).

In addition to these age-related degenerative and regenerative changes to myelin sheaths, there is an overall loss of myelinated nerve fibers. This has been reported in postmortem histological analyses of cerebral white matter in non-demented human subjects who show a decrease in the number of myelinated nerve fibers with age (Meirer-Ruge et al., 1990; Marner et al., 2003). One such study, a global stereological analysis of myelinated nerve fiber length, indicates that the overall length of nerve fibers in white matter decreases by as much as 10% per decade between the ages of 20 and 80 years (Marner et al., 2003). These findings from human autopsy material are further supported by electron microscopic studies of cerebral white matter in the rhesus monkey. Morphological analyses of the optic nerve, anterior commissure, and splenium of the corpus callosum of old monkeys reveal some cross-sectional profiles of myelinated axons with dense axoplasm, indicating that they are degenerating (Sandell and Peters, 2001; 2003; Peters and Sethares, 2002). The frequency of these degenerating axon profiles increase with age, and result in a loss of more than 40% of nerve fibers from the anterior commissure (Sandell and Peters, 2003) and optic nerve (Sandell and Peters, 2001), and a 25% loss of nerve fibers from the splenium (Peters and Sethares, 2002) over the lifespan of the rhesus monkey.

Recent *in vivo* analysis of the structural integrity of white matter in humans as measured by diffusion tensor magnetic resonance imaging (DT-MRI) suggests that white matter pathways may be differentially affected by aging, with frontal white matter being more affected than temporal and occipital white matter pathways (O'Sullivan et al., 2001; Salat et al., 2005; Yoon et al., 2008). For example, DT-MRI studies of the corpus callosum in humans indicate that the integrity of the genu decreases to a greater extent than the splenium (Head et al., 2004; Salat et al., 2005; Sullivan et al., 2006). Moreover, frontal lobe associated fiber tracts, such as the cingulate bundle, have been shown to be the earliest ones to be affected in normal aging (Yoon et al., 2008), and a recent DT-MRI study in the rhesus monkey has also found significant changes in white matter tracts associated with the prefrontal cortex, including the anterior corpus callosum, cingulate bundle, and superior longitudinal fascicle (Makris et al., 2007).

Together, the overall loss of myelinated nerve fibers and the alterations to their sheaths could result in the inefficient coordination and conduction of neuronal signals from the prefrontal cortex, contributing to some of the age-associated deficits in working memory, short-term memory, and executive system function observed with age in both humans (Albert, 1988;1993;Lamar and Resnick, 2004), and non-human primates (Presty et al., 1987;Moss et al., 1988;Rapp and Amaral, 1989;Moss et al., 1997; Moore et al., 2003;2006).

To date, the ultrastructural analysis of the affects of age on myelinated nerve fibers and their sheaths relating to the frontal lobe of the cerebral hemisphere has been limited to the

myelinated fibers within cortical area 46 of the dorsolateral prefrontal cortex, and to a lesser extent, those in the anterior commissure, which carries fibers from the orbitofrontal and anterior temporal cortices (Peters et al., 1994; Peters and Sethares, 2002; Sandell and Peters, 2003). The present study expands on these observations by quantifying the age-related deterioration of myelinated nerve fibers in the genu of the corpus callosum and the cingulate bundle: two pathways carrying nerve fiber projections from the dorsolateral prefrontal cortex. The genu of the corpus callosum is the major commissural pathway for the prefrontal cortex, while the cingulate bundle is a heterogeneous system of fibers connecting the prefrontal cortex, thalamus, striatum, cingulate gyrus, parietal cortex, and medial temporal lobe (Mufson and Pandya, 1984; Schmahmann and Pandya, 2006). The cingulate bundle is of particular interest due to its indirect and direct connections with the prefrontal cortex and medial temporal lobe (Goldman-Rakic et al., 1984; Morris et al., 1999); two brain regions critical for learning, memory, and executive system functions which are known to be impaired with advancing age (Goldman-Rakic, 1988; Miller and Cohen, 2001).

MATERIALS AND METHODS

Subjects

Twenty-one rhesus monkeys (*Macaca mulatta*), aged 4 - 32 years old, were used in this study (Table 1). Of these, seven were young (< 10 years), six were middle aged (10 – 20 years) and eight were old (> 20 years). Exact birthdates for two monkeys (AM023 and AM143) are not known and are approximated based on weight, dentition, and sexual maturity at the time they were entered into the study. Nineteen of the twenty-one monkeys have been involved in previous studies of age-related myelinated nerve fiber degeneration in the prefrontal cortex (Peters et al., 1994;Peters and Sethares, 2002), striate cortex (Peters and Nielsen, 2000;Peters et al., 2000), the splenium of the corpus callosum (Peters and Sethares, 2002), anterior commissure (Sandell and Peters, 2003), or optic nerve (Sandell and Peters, 2002), and are readily identified by their “AM” number. All animals were housed at facilities accredited by the Association for the Assessment and Accreditation of Laboratory Animal Care (AAALAC), with all care following the standards set by the National Institute of Health and the Institute of Laboratory Animal Resources’ Commission on Life Sciences’ *Guide for the Care and Use of Laboratory Animals* (1996). The Institutional Animal Care and Use Committee at Boston University approved all research protocols. All efforts were made to minimize the number of monkeys used, and their suffering.

Tissue Preparation

The protocol used for animal euthanasia and tissue fixation has been previously reported in detail (Peters et al., 1994). Briefly, each monkey was anesthetized to a state of areflexia, intubated, and respirated with a mixture of 5% CO_2 and 95% O_2. The chest cavity was opened, and the monkey perfused intra-aortically with a warm (37°C) mixed-aldehyde solution containing 1% paraformaldehyde and 1.25% glutaraldehyde in 0.1M sodium cacodylate or phosphate buffer at a pH of 7.4. The brain was removed, weighed, and hemisected. One hemisphere was selected for processing for electron microscopic analysis. This hemisphere was post-fixed in cold (4°C) 2% paraformaldehyde and 2.5% glutaraldehyde in the same buffer used for the perfusion, and stored in this solution until two-millimeter thick tissue blocks were removed from the cingulate bundle and genu of the corpus callosum.

For the cingulate bundle, tissue blocks containing the cingulate gyrus, underlying white matter, and adjacent body of the corpus callosum were taken at the anterior/posterior level of the anterior commissure. For the genu of the corpus callosum, blocks were removed from its dorsal half. Blocks were post-fixed in 1% osmium tetroxide, dehydrated, embedded in

Araldite resin in a BEEM capsule, and polymerized at 37°C for three days. From each embedded tissue block, 1μm thick sections were cut using an MT-6000 XL ultramicrotome (RMC Inc.; Tucson, AZ), and stained with 1% toluidine blue. Sections through the cingulate cortex and white matter were cut in the coronal plane, while sections through the genu of the corpus callosum were cut in the sagittal plane.

In toluidine blue stained, semi-thick sections, the dorsal genu of the corpus callosum is clearly discernible. In contrast, the cingulate bundle is difficult to identify, but is clearly apparent in fixed, unstained tissue (Fig. 1). To facilitate its identification in stained sections, a tracing of the cingulate bundle was made from the face of an adjacent unstained, and unembedded tissue block at 40x magnification using a camera lucida. This tracing was then superimposed on a 40x magnification tracing of the 1μm thick, toluidine blue stained plastic section in order to locate the cingulate bundle. With each structure clearly delineated, thin sections were taken and mounted onto 300 mesh Formvar/carbon coated copper grids, stained with uranyl acetate and lead citrate, and examined in a JEOL 100S electron microscope (JEOL USA Inc.; Peabody, MA).

Quantification of Myelinated Nerve Fiber Number Per Unit Area

Thin sections were systematically randomly sampled at a magnification of 6,000x by taking electron micrographs at the centers of grid squares. For the cingulate bundle, sampling was conducted with a fixed horizontal and vertical periodicity of every third grid square, yielding 13 to 21 micrographs per section. For the genu, a periodicity of every fourth grid square was used, yielding 9 to14 micrographs per section. Micrographs were printed to a final magnification of 14,250x.

A counting frame of fixed x/y dimensions was centered over each print, and myelinated and unmyelinated nerve fiber profiles were counted using the axon profile as the counting object, following the inclusion/exclusion criteria of the unbiased counting frame (Gundersen, 1977). Only cross-sectional profiles of nerve fibers were sampled in both fiber tracts. After adjusting for magnification, the number of cross-sectional myelinated and unmyelinated nerve fiber profiles per unit area (area number density) were computed by dividing the total number of profiles counted by the total area examined.

Quantitative Analysis of the Morphology of Myelinated Nerve Fiber Profiles

The morphology of each myelinated nerve fiber profile included in the quantitative analysis of fiber area number density was further characterized as being a cross-section through an internode, paranode, or node of Ranvier, based on established morphological criteria (Peters et al., 1991, Rosenbluth, 1995). Profiles were also examined to determine if there were age-related changes in their axons or myelin sheaths. Characterizations of each nerve profile were initially made by one author (M.P.B), then reviewed and agreed upon by a second author (A.P.). A minimum of 1000 profiles was counted in the cingulate bundle and 1300 profiles in the genu for each subject. Morphological changes in myelin sheaths and in axons are expressed as a percentage of the total number of nerve fiber profiles examined. Representative micrographs prepared for publication were scanned into a computer, adjusted for brightness and contrast, and stored using Adobe Photoshop CS software (Adobe Systems Inc., San Jose, CA).

Caliber of Myelinated Axons

Nerve fibers with normal myelin sheaths were measured to determine if axonal diameter changes with age or is associated with observed alterations in myelin sheath structure. An unbiased counting frame, centered over each electron micrographic print, was used to sample myelinated nerve fiber profiles, with at least 250 cross-sectioned nerve fibers

sampled from each subject for both the cingulate bundle and genu. Axon profiles were outlined on sheets of acetate, and the drawings subsequently digitized using PhotoStudio software and a Canon Canoscan 1300 scanner. The area of each outlined axon profile was calculated using NIH Image version J software, devolved to a circle, and the diameter determined. Axon profiles from each subject were organized into one of six bins, 0.4μm in width, from less than 0.4μm to greater than 2.0μm, and then divided by the total area examined, to yield the number of fibers per unit area for each caliber class. To further assess the relationship between axon diameter and myelin sheath alterations, the axon of every identified nerve fiber profile with an altered myelin sheath was traced onto acetate, its diameter estimated, and the percentage of degenerative and redundant myelin sheath alterations determined for each caliber class of myelinated nerve fibers.

Cross Sectional Area of the Cingulate Bundle and Corpus Callosum

To determine if there are changes in the cross-sectional area of the cingulate bundle with age, the white matter under the cingulate gyrus was traced from 1μm thick, coronal sections stained with toluidine blue. The boundaries of the cingulate white matter are diagrammed in Figures 1A and 1B. At the level of the anterior commissure, the cingulate white matter is bounded on its dorsal, medial, and lateral aspects by the gray matter of the cingulate gyrus. Ventrally, it is bounded by the transversely running fibers of the body of the corpus callosum. Its inferolateral boundary was arbitrarily defined by a line oriented perpendicular to the cingulate sulcus, from the gray matter/white matter boundary dorsally, to the underlying corpus callosum ventrally. As defined, this cross-sectional area includes the more ventrally placed cingulate bundle as well as the surrounding local system fibers beneath the cortex. Each section was viewed at 20x magnification with a computer-assisted light microscope and StereoInvestigator version 6.0 software (MicroBrightField Inc.; Williston, VT). The white matter underlying the cingulate cortex was traced, and its area was calculated by the software program using the x and y coordinate of each pixel that formed the drawn contour.

To address possible age-related changes in the size of the genu of the corpus callosum, photographs of the mid-sagittal surface of 24 rhesus monkey brains, ranging from 4 to 30 years of age, were used. Photographs were available for only nine of the eighteen brains used in this study (Table 2), and of these nine; the old age monkeys in the subject set were limited to two females. Therefore, to more accurately determine the effects of age on genu size, available photographs from fifteen additional subjects, involved in an ongoing study of the neurobiological basis of cognitive decline, were included in the analysis. All 24 monkeys had been perfused with 1% paraformaldehyde and 1.25% glutaraldehyde in 0.1M sodium cacodylate or phosphate buffer, hemisected, and the mid-sagittal face digitally photographed. Each photograph was printed using a Kodak PS 8650 color printer, and the cross-sectional area of the corpus callosum in its entirety traced onto a sheet of acetate. Tracings were then scanned into a Power Macintosh 8650/300 using an Agfa Arcus II scanner. The genu of each corpus callosum was defined following criteria established by Witelson (1989), in which the callosum is divided into seven regions based on the origin and topography of cortical inter-hemispheric fibers. In mid-sagittal section, the genu is the most anterior part of the corpus callosum. The posterior boundary of the genu is defined as a straight line, perpendicular to the long axis of the corpus callosum, at the boundary of the corpus callosum with the anterior tip of the septum pellucidum (Fig. 1C). The cross-sectional area of each genu was then calculated using NIH Image J software.

Behavioral Assessment

Twenty of the twenty-one rhesus monkeys used in this study had been administered a series of behavioral tasks to assess their cognitive ability prior to being euthanized (Table 1). This

battery included acquisition and two delay phases of the Delayed Non-Match to Sample (DNMS) task as well as the spatial and object versions of the Delayed Recognition Span Task (DRST). Detailed descriptions of each of these behavioral tasks have been presented previously (Moss et al., 1988;Moss et al., 1997).

All twenty behaviorally tested monkeys completed acquisition of the DNMS task, a test of rule learning. A 2-minute delay phase of the DNMS was administered to nineteen monkeys, and a 10-minute delay phase to thirteen monkeys: both tests of short-term memory. The DRST, a test of working memory load, was administered as both spatial and object versions. Nineteen monkeys completed the spatial version and fourteen monkeys completed the object version of the DRST.

The combined performances by each of nineteen monkeys that completed the DNMS Acquisition, DNMS 2-minute delay, and the DRST Spatial tasks were normalized to the performance of fifty-three adult monkeys as described by Herndon et al. (1997), resulting in a composite score of global cognitive impairment, the CII, or Cognitive Impairment Index. The CII is used here as a measure of the animal's overall cognitive decline with age. The larger the value of the CII, the greater a subject's overall impairment.

Data Analysis

The associational strengths between variables of myelinated nerve fiber integrity, behavioral performance, and age were analyzed using the Pearson product-moment correlation coefficient with a linear fit. For the analysis of age as an independent variable, additional piecewise linear models were used to assess non-linear relationships between variables of myelinated nerve fiber degeneration and age. This analysis estimates separate linear slopes for three-age intervals: young (<10 years), middle aged (10 - 20 years), and old (>20 years). Within each of these groups, the regression coefficient (b) denotes the rate of change of the variable being measured as a function of age. These age intervals were selected prior to performing any statistical analyses, and are based on theoretical grounds.

Additional analyses were conducted using Pearson product-moment correlation coefficients with a linear fit, or for between-groups comparisons, the Student's pair-wise t-test. Associations with p-values less than 0.05 were deemed statistically significant. In the following text and tables, data are presented as the mean plus or minus the standard deviation.

RESULTS

The cingulate bundle and the genu of the corpus callosum are largely comprised of myelinated nerve fibers, and interspersed amongst them are unmyelinated nerve fibers, along with the cell bodies and processes of oligodendrocytes, astrocytes, and microglial cells. The cingulate bundle and genu have a similar composition, with 82% of axons being myelinated in the cingulate bundle and 81% in the genu. Representative electron micrographs of the cingulate bundle are given in Figures 2 and 3. Typically, the profiles of myelinated nerve fibers in young monkeys (Fig. 2) are tightly packed, with the myelin sheaths of adjacent fibers often abutting one another. Unmyelinated nerve fibers (Fig. 2 and 3; U) occur either singly or in groups scattered amongst the more numerous myelinated nerve fiber profiles. In contrast, myelinated nerve fiber profiles in older monkeys (Fig. 3) are more widely separated, with numerous processes of astrocytes (Fig. 3; As) occupying the spaces between them.

Numbers of Myelinated Nerve Fibers per Unit Area with Age

As determined from electron micrographs of the cingulate bundle and genu of the corpus callosum, the number of myelinated nerve fibers per unit area decreases with age (Table 2). In the cingulate bundle, the mean number of profiles per $100\mu m^2$ decreases from 63 ± 8 in young monkeys, to 56 ± 4 in middle age, and 49 ± 9 in the old monkeys. The more tightly packed nerve fibers in the genu of the corpus callosum show a similar age-related decrease in area number density, with the mean number of myelinated nerve fibers per $100\mu m^2$ decreasing from 99 ± 12 fibers in the youngest monkeys, to 77 ± 15 in middle age, and 84 ± 13 fibers in old age. Using a linear fit, the number of myelinated nerve fiber profiles per $100\mu m^2$ is negatively correlated with age in both pathways (Cingulum: $r = -0.647$, $p < 0.005$; Genu: $r = -0.480$, $p < 0.05$). Overall, there is a similar decrease of about 20% in myelinated nerve fiber area number density between the ages of 6 and 30 years in both structures. As shown in Figure 4A, piecewise linear analysis indicates that the decreases in the number of myelinated nerve fibers per unit area occur gradually with age, and do not exhibit a significant age-group specific decrease in either pathway.

In contrast to the age-related reduction in the number of myelinated nerve fibers per unit area, the number of unmyelinated axons per unit area is not significantly altered with age in either the cingulate bundle ($r = 0.408$, $p = 0.0829$) or genu ($r = -0.090$, $p = 0.7141$). Additionally, piecewise linear analysis indicates that there are no significant age-group specific changes in the area number density of unmyelinated axons in either structure.

Degeneration of Myelinated Axons with Age

The normal profile of an axon of a myelinated nerve fiber shows an electron-lucent axoplasm containing mitochondria and an array of microtubules and neurofilaments. Evidence of the degeneration of the axons of myelinated nerve fibers is indicated by the appearance of axonal profiles with a darkened axoplasm (Lampert, 1967). Such degenerating axons are found in both middle aged and elderly monkeys and often contain vacuoles and dense debris (Fig. 5). Further evidence for frank axonal degeneration is the presence of empty myelin sheaths.

At any age, the frequency of degenerating axonal profiles in the cingulate bundle and genu is less than 1% of the total myelinated nerve fiber population, but even in this small range, the frequency of degenerating axon profiles significantly increases with age in both the cingulate bundle ($r = 0.857$, $p < 0.0001$) and the genu ($r = 0.853$, $p < 0.0001$). Based on piecewise linear analyses, the age-related increase in degenerating axon profiles is greatest during middle age in both structures (Cingulum: $b = 0.040$, $p < 0.05$; Genu: $b = 0.050$, $p < 0.005$; Fig. 4B).

Size of Myelinated Axons: Relationship to Area Number Density

To determine if any group of myelinated nerve fibers is more prone to degeneration than another, the mean diameter of their axons was determined in both the cingulate bundle and genu. Across all age groups the mean diameter of cingulate bundle axons is 0.67μm ± 0.06μm in young, 0.70μm ± 0.05μm in middle age, and 0.66μm ± 0.03μm in old subjects, as compared to 0.58μm ± 0.04μm, 0.62μm ± 0.05μm, and 0.57μm ± 0.04μm in the genu, so that neither structure shows a significant change in the mean diameter of myelinated axons with age. Consequently, the decrease in the number of myelinated nerve fibers per unit area observed in both structures with age is not the result of an age-related increase in the diameter of those myelinated axons.

An analysis of the number of myelinated nerve fibers per unit area, by separating myelinated axons from each subject into six caliber classes of 0.4μm, from < 0.4μm to > 2.0μm, showed

no evidence for a class specific loss of nerve fibers with age. When analyzed individually, the number of myelinated nerve fibers per unit area in each of the six diameter classes showed no significant change with age in either the cingulate bundle or genu of the corpus callosum.

Cross-Sectional Area of Cingulate White Matter and Genu of the Corpus Callosum

The cross-sectional area of the cingulate white matter from all eighteen subjects shows no significant change with age ($n = 18$; $r = 0.014$, $p = 0.9546$). When males ($n = 9$) and females ($n = 9$) are considered separately, the area of the cingulate white matter is not statistically altered with age in female monkeys ($r = 0.472$, $p = 0.1684$.), but exhibits a 28% decrease in male monkeys ($r = -0.661$, $p < 0.05$). This finding is significant in that a loss of cross-sectional area occurring concurrently with a decrease in myelinated nerve fibers may result in an overall under estimation of myelinated nerve fiber loss from the cingulate bundle with age in males. The mid-sagittal area of the genu is not significantly altered with age ($n = 24$, $r = -0.080$, $p = 0.7038$), nor is a difference detected when males ($n = 16$) and females ($n = 8$) are considered separately.

Age-Related Deterioration of Myelin Sheaths

In both the cingulate bundle and genu, the majority of myelinated nerve fiber profiles have compact myelin lamellae, although some of the sheaths show focal “shearing” defects, which are considered to be artifacts of tissue processing. Shearing defects appear as local patches where adjacent lamellae become detached from one another, resulting in wisps of myelin separated by small empty spaces that either project inward to indent the axon, or bulge outward from the surface of the myelin sheath (Fig. 2, arrows).

Distinct from artifacts of tissue processing, are degenerative or dystrophic alterations in myelin sheaths. These become more frequent with age, and can be classified into three types: dense sheaths, myelin balloons, and redundant sheaths. Dense sheaths and myelin balloons are considered to be evidence of myelin sheath degeneration. Dense sheaths result from splits at the major dense line that are filled with electron dense cytoplasm (Fig. 3, 5). Frequently, this dense cytoplasm contains vacuoles and dense amorphous bodies. Since the major dense line is produced by the apposition of the inner leaflets of an oligodendrocyte’s plasma membrane, the dense cytoplasm seen in the sheaths of some nerve fibers from middle aged and old monkeys must be derived from the oligodendrocyte that forms the sheath. Dense sheaths are the most common form of myelin sheath defect observed in both the cingulate bundle and genu, accounting for 50-80% of age-related myelin sheath alterations.

Myelin balloons (Fig. 3) arise from a splitting of the myelin sheath at the intraperiod line. These balloons appear as spherical bulges of the sheath that are filled with fluid (Feldman and Peters, 1998). Since the intraperiod line represents the apposition of the outer faces of the oligodendrocyte plasma membrane in adjacent turns of the sheath, the cavity forming a myelin balloon is continuous with the extracellular space, and this may be the origin for the fluid filling a balloon. Myelin balloons are common in aging gray matter (Peters and Sethares, 2002), but they are rare in white matter tracts such as the genu and cingulate bundle, accounting for less than 3% of all abnormal myelin sheath profiles.

Redundant sheaths are myelin sheaths that are too large for the axon they ensheath (Rosenbluth, 1966). In a cross-sectional profile, the axon is typically situated at one end of a sheath profile, with the redundant myelin looping away from it (Fig. 6). It has been suggested that these irregular myelin profiles may result from the active formation of myelin (Rosenbluth, 1966) or the remodeling of myelin sheaths (Cullen and Webster, 1979) in the

central nervous system. Redundant sheaths vary in frequency in the genu and the cingulate bundle, but typically account for 20-50% of the observed age-related myelin sheath changes.

While alterations in myelin sheath structure are present at every age, they are much more prevalent in middle aged and old animals. The frequency of all altered myelinated nerve fiber profiles increases significantly with age in both the cingulate bundle ($r = 0.953$, $p < 0.0001$) and genu ($r = 0.953$, $p < 0.0001$). Further, piecewise linear analysis indicates that this age-related increase in altered myelin sheaths occurs most commonly in middle and old aged monkeys (Fig. 7A). In the genu, the sharpest increases occur in middle age ($b = 0.489$, $p < 0.0001$), and in the cingulate bundle, it occurs in old monkeys ($b = 0.372$, $p < 0.0001$). Individually, the frequencies of myelinated nerve fibers with dense sheaths (Cingulum: $r = 0.943$, $p < 0.0001$; Genu: $r = 0.945$, $p < 0.0001$) or myelin balloons (Cingulum: $r = 0.584$, $p < 0.01$; Genu: $r = 0.543$, $p < 0.05$) positively correlate with age in both structures. In contrast, redundant sheaths increase significantly with age in the cingulate bundle ($r = 0.545$, $p < 0.05$) but not in the genu of the corpus callosum ($r = 0.299$, $p = 0.2137$.). Piecewise analysis of data from both the genu and cingulate bundle shows that the frequency of dense sheaths rapidly increases after 10 years of age (Fig. 7B), while redundant sheaths increase significantly between 10 and 20 years of age, but thereafter maintain a plateau, or decrease in frequency (Fig. 7C).

Size of Myelinated Axons: Relationship to Myelin Sheath Alterations

To determine if alterations in myelin sheaths preferentially affect axons of a particular diameter, the frequency of alterations was calculated for six caliber classes of axons, from < 0.4μm to > 2.0μm, using the combined data from the middle aged and old monkeys. In the cingulate bundle and genu, the degenerative changes in myelin sheaths, such as dense sheaths and myelin balloons, are present on nerve fibers of all sizes, but are more frequent in larger caliber fibers (Fig. 8; A and B). Conversely, in both fiber tracts, the redundant sheaths predominate in nerve fibers of a smaller caliber, and are absent in the largest caliber nerve fibers (> 1.6μm).

Continuing Myelination in the Aging Brain

As pointed out earlier, redundant sheaths are considered to be evidence of the active myelination of nerve fibers (Rosenbluth, 1966; Cullen and Webster, 1979). In addition to these redundant sheaths, some myelinated nerve fibers of both the cingulate bundle and genu show evidence of early stages of myelination, so that in older monkeys, some fibers have inappropriately thin myelin sheaths composed of only two or three layers of myelin (Fig. 9). Such thin myelin sheaths are generally regarded as an indicator of remyelination in the central nervous system (Gledhill and McDonald, 1977; Ludwin, 1978; 1981; Hirano, 1989).

Internodes, Paranodes, and Nodes of Ranvier

A further indicator of continuing myelination in the aging CNS is the presence of short internodal lengths of myelin (Gledhill and McDonald, 1977; Ludwin, 1978; 1981; Hirano, 1989). Each length of myelin can be considered to have two distinct domains: a central domain of compact myelin, and paranodal domains at the two ends of each length of myelin where the myelin lamellae terminate adjacent to nodes of Ranvier. Cross-sectional profiles through the central portion of each internodal length of myelin are identified by compact myelin lamellae and a distinct separation between the innermost plasma membrane of the oligodendrocyte and the axolemma (Fig. 5; I). In contrast, at a paranode there is a continuous ring of cytoplasm separating the axon from the inside of the compact myelin sheath, and the plasma membranes of the innermost turn of the oligodendrocyte process and the axon are in close apposition, forming a complex junction (Fig. 5; P).

At the node of Ranvier, the axon is bare (Fig. 2; N). The characteristic feature of a nodal profile is the presence of a dense undercoating on the inner surface of the axolemma. This undercoating is essential for the accurate identification of nodes, and when it is not apparent, it is not possible to distinguish nodal profiles from those of unmyelinated nerve fibers.

With increasing age, linear analysis shows that the frequency of profiles through paranodes significantly increases in both the genu of the corpus callosum ($r = 0.780$, $p < 0.0001$) and the cingulate bundle ($r = 0.523$, $p < 0.05$). Inversely, internodal profiles significantly decrease with age in both regions (Genu: $r = -0.766$, $p < 0.0001$; Cingulum: $r = -0.462$, $p < 0.05$). Profiles through nodes of Ranvier are rare in both structures, and given this, no significant change in their frequency is observed with age (Genu: $r = -0.050$, $p = 0.8389$; Cingulum: $r = 0.061$, $p = 0.8041$).

Piecewise, linear analysis of the frequency of paranodal profiles with age indicates that the increase in their frequency mainly occurs after 20 years of age in the genu ($b = 0.311$, $p < 0.005$; Fig. 10), and there is a trend toward a significant increase in the same age group in the cingulate bundle ($b = 0.160$, $p = 0.0961$; Fig 10). Together, the increase in frequency of paranodal profiles, and the decrease in internodal profiles indicates that there is an increase in the total number of internodal lengths of myelin, and provides further evidence that there is remyelination of some axons in older monkeys.

Correlations with Cognitive Performance

The individual performance of each of the twenty monkeys that underwent behavioral testing is given in Table 1. Overall, these monkeys show age-related deficits in performance on tasks of rule learning (DNMS Acquisition), and short-term recognition memory (DNMS 2-Minute Delay). Aging is associated with poor performance on acquisition of the DNMS task as evidenced by an increased number of trials to criterion ($r = 0.548$, $p = 0.01$). On the 2-minute delay phase of the DNMS task, increasing age is associated with a reduced number of correct responses ($r = -0.487$, $p < 0.05$). Scores on the 10-minute delay phase of the DNMS task and on both versions of the DRST do not correlate with age. Based on the combined scores on the acquisition and 2-minute delay phase of the DNMS and the spatial versions of the DRST, a measure of global cognitive ability, the cognitive impairment index (CII), is calculated. Using a linear fit, CII increased significantly with advancing age ($r = 0.539$, $p < 0.05$), indicating increasing impairment with age.

Statistical correlations between ultrastructural changes in the genu of the corpus callosum and behavioral performance from seventeen monkeys reveal little relationship between age changes in the myelinated nerve fibers of the genu and cognitive function. There is only one significant association; that between the percentage of myelinated nerve fiber profiles with degenerating axons and the percentage of correct responses on the 2-minute delay phase of the DNMS Task ($n = 16$, $r = -0.510$, $p < 0.05$).

In marked contrast, the eighteen monkeys used for analysis of the cingulate bundle show a number of significant associations between alterations in myelinated nerve fiber morphology and cognitive performance. The percentage of myelinated nerve fiber profiles with degenerating axons is negatively associated with performance on the acquisition of the DNMS task ($n = 18$, $r = 0.702$, $p < 0.001$), and the 2-minute delay phase of the DNMS task ($n = 17$, $r = -0.660$, $p < 0.005$). As shown in Figure 11A, global cognitive impairment also increases with the increasing frequency of degenerating axons in the cingulate bundle ($n = 18$, $r = 0.688$, $p < 0.005$). The frequency of degenerating axons does not correlate with performance on the 10-minute delay phase of the DNMS, or on either the spatial or object versions of the DRST.

In the cingulate bundle, the frequency of nerve fibers with altered myelin sheaths also shows significant associations with behavioral performance. An increase in the percentage of nerve fibers with altered myelin sheaths is significantly correlated with poorer performance on acquisition of the DNMS task ($n = 18$, $r = 0.704$, $p < 0.0005$), and DNMS 2-minute delays ($n = 17$, $r = -0.472$, $p < 0.05$). As shown in Figure 11B, myelin sheath alterations in the cingulate bundle are also positively associated with CII ($n = 18$, $r = 0.709$, $p < 0.001$). The frequency of altered myelin sheath profiles in the cingulate bundle does not correlate with performance on the 10-minute delay phase of the DNMS, or with either version of the DRST.

The number of myelinated nerve fibers per unit area, percentage of paranodal profiles, and percentage of internodal profiles in the cingulate bundle are not significantly associated with performance on any individual behavioral task, or with overall cognitive impairment.

DISCUSSION

This study has examined the affects of age on the myelinated nerve fibers in the cingulate bundle and genu of the corpus callosum. With increasing age, there is a marked deterioration in the structure of some myelinated nerve fibers in each pathway. This deterioration begins, and is most pronounced, in middle age, with structural alterations in myelin sheaths that include the accumulation of dense cytoplasm in some sheaths, and the ballooning of other sheaths. Such alterations affect 4% to 7% of myelin sheaths in monkeys over 20 years of age. There is also a significant age-related decrease in the area number density of myelinated, but not unmyelinated, nerve fibers in both pathways.

Even though some sheaths of myelinated nerve fibers in the cingulate bundle and genu degenerate with age, there is also evidence for the remyelination. This is supported by the presence, in middle and old aged monkeys, of some myelinated nerve fiber profiles that have inappropriately thin myelin sheaths, as well as some with redundant myelin. Further evidence for remyelination in the cingulate bundle and genu of the corpus callosum with age is an increase in the frequency of paranodal profiles, suggesting that the average internodal length of myelin is decreasing, and the total number of internodal lengths of myelin is increasing.

Methodological Considerations

In this study we assessed the number of myelinated fibers using two-dimensional (2D) counting frames oriented perpendicular to the long axis of the cingulate bundle and the genu of the corpus callosum. For both structures, we estimated the total cross sectional area and the total number of myelinated fibers within that area to obtain a fiber density measure. In reporting a density measurement, it is important to determine whether or not the denominator (total cross-sectional area of the fiber tract) has changed as shrinkage of the tract area without a change in the number of fibers would manifest as an increased density, while an expansion of the tract area without change in number would manifest as an decrease in density. In the present study we observed that there was no significant change in the total cross-sectional area of either fiber tract with age but there was a decrease in the number of myelinated nerve fiber profiles per unit area. Hence the age-related decrease in the number of nerve fibers per unit area is not an artifact of a change in the cross-sectional area of the tract.

It is also important to consider whether changes in the third, or z-dimension, of each tract could affect these measures. The myelinated fibers in each tract run for long distances in the z-dimension (anterior to posterior for the cingulate bundle and medial to lateral for the genu of the corpus callosum) and have a variety of origins and terminations, making it impossible

to determine the lengths of the tracts. In this regard, the 2-D sampling done orthogonal to the fiber trajectories (i.e to the z-dimension) would not be affected by either shrinkage or expansion of the length of the fiber tract.

Finally, in support of our contention that there is a loss of nerve fibers, there is the evidence that some nerve fibers degenerate with age (Fig 5), and it should be noted that more global 3D measures of total myelin with *in vivo* MRI methods by both this group (Wisco et al., 2008) and others (Guttmann et al., 1998;Allen et al., 2005) have shown that total cerebral white matter volume decreases with age. Hence, the observed age-related decrease in the numbers of myelinated nerve fibers per unit area in both the cingulate bundle and genu reported here is best explained as a loss of nerve fibers.

Loss of Nerve Fibers with Age

While a number of studies using MRI have described age-related losses of white matter in the forebrain of humans (Guttmann et al., 1998; Allen et al., 2005), there are only a few studies that provide histological data on the loss of white matter and/or axons with age in the human brain. In one study, stereological methods were used to quantify the total length of myelinated nerve fibers in the cerebral white matter of non-demented aging humans using systematic random sampling of biopsy specimens (Marner et al., 2003). This study reported that the total length of myelinated fibers shortens by as much as 45% between the ages of 20 and 80 years.

In the rhesus monkey, as in humans, *in vivo* MRI studies have demonstrated a significant loss of white matter volume with age (Wisco et al., 2008). In addition, numerous studies provide histological evidence of age-related losses of myelinated nerve fibers in a number of different structures. In the optic nerve (Sandell and Peters, 2001) and the anterior commissure (Sandell and Peters, 2003), age-related decreases in myelinated nerve fiber number have been estimated to be 44% and 50% respectively.

In the present study, the two-dimensional quantification of the number of myelinated nerve fibers per unit area in the genu and cingulate bundle shows that there is a significant decrease in fibers numbers with age. Given that there is no change in the cross-sectional area of either fiber tract with age, it can be concluded that the observed decreases in area number density represent a loss of nerve fibers with age. Compared to the fiber tracts studied previously, this loss of myelinated nerve fibers is less robust. For the cingulate bundle, the average myelinated nerve fiber loss is 22% between the ages of 6 and 30 years, while the genu shows a 21% loss.

What brings about this loss of nerve fibers? There is little evidence for any significant loss of neurons in normal aging in either the human (e.g. Terry et al., 1987; Pakkenberg and Gundersen, 1997) or the monkey brain (e.g. Morrison and Hof, 1997; Peters et al, 1998; Peters and Rosene, 2003). The dorsal aspect of the genu of the corpus callosum, which was analyzed in this study, contains long projection axons from layer III neurons of prefrontal cortical areas 9, 12, and 46 (Barbas and Pandya, 1984; Pandya and Rosene, 1985), as well as from anterior parts of the cingulate cortex (Schmahmann and Pandya, 2006). Neuron counts from area 24 of the anterior cingulate gyrus in humans (Gittins and Harrison, 2004) and area 46 along the banks of principal sulcus in the rhesus monkey (Peters et al., 1994; Smith et al., 2004) have shown no significant loss of neurons with age. However, it should be noted that even though they observed no change in neuron number in adjacent area 46, Smith et al. (2004) reported a significant 32% reduction in Nissl stained neurons from the cortical area 8a. Commissural fibers from area 8a course through the rostral part of the body of the corpus callosum, immediately posterior to the fibers of the dorsal genu. If there is a loss of neurons

from area 8a, it is possible that a small fraction of the nerve fiber loss in the genu is the consequence of this reduction in neuron number.

Even less information exists about the affects of age on the neurons contributing axons to the cingulate bundle. The cingulate bundle is a complex intrahemispheric fiber bundle composed of nerve fibers from dorsolateral prefrontal, medial prefrontal, orbitofrontal, cingulate, retrosplenial, parietal, entorhinal, and parahippocampal cortices, along with the presubiculum, striatum and thalamus (reviewed in Schmahmann and Pandya, 2006). Beyond the studies from the prefrontal and cingulate cortices noted above, the one relevant area that has received particular attention is the entorhinal cortex, which, like the prefrontal cortex, plays a role in learning and memory processes. Studies of the entorhinal cortex in the rhesus monkey have found no loss of neurons with age (Gazzaley et al., 1997; Merrill et al., 2001). A study of presubicular neuron number in non-demented humans also revealed no loss of neurons with age (Harding et al., 1998). So again, neuron degeneration is not likely to be a major contributor to the loss of myelinated nerve fibers from the aging cingulate bundle.

Interestingly, there appears to be little loss of nerve fibers from the intracortical bundles of axons found in primary visual cortex (Nielsen and Peters, 2001). Consequently, as proposed by Peters and Rosene (2003), a likely explanation for the loss of myelinated nerve fibers from cerebral white matter may be the selective degeneration of the long projecting axons of cortical neurons with age. In such a scenario, cortical neurons would be maintained and receive trophic support from rich, local, intracortical axon plexuses, despite the “dying back” of their long projecting axons.

In addition to the estimated 45% decrease in total myelinated nerve fiber length across the adult human lifespan discussed above, Marner and colleagues (2003) further reported a 13% increase in the mean diameter of myelinated axons over this same age range, leading the authors to conclude that smaller nerve fibers are being lost with age. In agreement with this histological data, recent DT-MRI studies suggest that a preferential loss of small diameter fibers can account for age-related inconsistencies in the correlations between indirect measures of white matter integrity such as fractional anisotropy and apparent diffusion coefficients (Yoon et al., 2008). However, in the present study of the genu and cingulate bundle, no evidence was found to suggest that a particular caliber of axons is preferentially lost with age.

Deterioration of Myelin Sheaths with Age

Age-related alterations in myelin sheaths have been previously observed in the monkey visual cortex (Peters et al., 2000), prefrontal cortex (Peters and Sethares, 2002), optic nerve (Sandell and Peters, 2001), anterior commissure (Sandell and Peters, 2003), and splenium of the corpus callosum (Peters and Sethares, 2002). In each of these areas the frequency of alterations increased with age. Similarly, the cingulate bundle and genu of the corpus callosum show a marked increase in the frequency of myelin sheath alterations with age. In young monkeys, only a small percentage (< 2%) of fibers show alterations in their myelin sheaths, but by middle age the frequency of alterations steadily increases, so that in old age, 6-9% of myelin sheaths profiles show alterations.

The most frequent form of myelin sheath alteration is a splitting of the sheath to accommodate dense cytoplasm. Similarly disorganized, dense cytoplasm has been described in the soma as well as internal and external tongue processes of oligodendrocytes exposed to toxins (Ludwin, 1978), or pathogenic viruses (Powell et al., 1975; Blakemore et al., 1988).

Although they are relatively infrequent in the cingulate bundle and genu, the presence of myelin balloons provides further evidence for the degeneration of myelin sheaths with age.

The fluid-filled vacuolization of the myelin sheath is a common sign of myelin sheath degeneration in experimentally induced animal models of demyelination secondary to toxin exposure (Wisniewski and Raine, 1971; Blakemore, 1972; Blakemore et al., 1972; Ludwin, 1978) or in experimental disease states such as experimental allergic encephalomyelitis (EAE) (Raine et al., 1969). In experimental cases, the induced demyelination may be due to both direct damage to the myelin sheath or the indirect result of oligodendrocyte damage, but the precipitating event that leads to degenerative myelin sheath alterations in the aging cingulate bundle and genu remains unknown. Interestingly, a recent study in aging rats has shown that some oligodendrocytes undergo apoptosis with age (Cerghet et al., 2006), suggesting that degenerative myelin sheath alterations in aging may result from death of the parent oligodendrocyte.

Remyelination

Although there is ample evidence for the degeneration of myelin sheaths in the aging monkey brain, there are also indications that some nerve fibers are actively remyelinating. As previously shown in the primary visual cortex and anterior commissure of the rhesus monkey, aging is accompanied by an increased frequency of paranodal profiles, and decreased frequency of internodal profiles, indicating a shortening of internodes and an overall increase in the total number of internodal lengths of myelin (Peters et al., 2001; Sandell and Peters, 2003). There is a similar increase in paranodal profile frequency in the genu of the corpus callosum, with a trend toward a significant increase in the cingulate bundle. Additionally, in middle age, there is an increase in the frequency of redundant myelin sheaths, which may indicate continuing myelination (Rosenbluth, 1966), or as the active remodeling of myelin sheaths (Cullen and Webster, 1979).

Recent studies indicate that the overall capacity for the old brain to remyelinate may be limited. Studies in the rat have found a decreased capacity for remyelination in old age following experimental, toxin induced demyelination (Hinks and Franklin, 2000; Sim et al., 2002; Irvine and Blakemore, 2006; Shen et al., 2008). The present results are equivocal. In agreement with these studies, the frequency of redundant myelin sheaths follows a unique temporal pattern with age as compared to other myelin sheath changes: predominating in middle age, and thereafter maintaining a plateau or decreasing in frequency in older animals. By contrast, the frequency of paranodal profiles, representing the result of remyelination, is increased in old but not middle aged monkeys. Of note, a study by Li and colleagues (2006) has shown that deficiencies in remyelination occur to a greater extent in old male rats as compared to old female rats. Five of the six middle age monkeys used in the present study were male. The impact that this male-weighted subject set may have on the present findings is unclear, but may serve to underestimate the overall frequency of paranodal profiles and redundant myelin sheaths in this age group, and possibly overestimate the frequency of degenerative myelin sheath changes in these same subjects.

An additional factor regulating the remyelination of deteriorating nerve fibers may be axon diameter. Studies of cuprizone-induced demyelination in mice have found that the spontaneous remyelination of demyelinated lesions preferentially involves axons that are less than 1μm in diameter (Mason et al., 2001). The present analysis shows that small caliber axons are most likely to be ensheathed by redundant myelin, as redundant sheaths around axons greater than 1.2μm in diameter are rare.

Contributions to Cognitive Decline

The age-related degeneration of myelinated nerve fibers likely results in impairments in cognition function through a disruption in the coordination and conduction of neuronal signals between brain regions. In support of this notion, electrophysiological studies

measuring axon conduction velocity in the spinal cord of cats have shown a significant slowing in velocity with age (Morales et al, 1987; Xi et al., 1999). Furthermore, previous electron microscopic analyses of myelinated nerve fiber deterioration in the aging rhesus monkey have found significant associations between the increased frequency of altered myelin sheaths in the primary visual and prefrontal cortices and poor performance on cognitive tasks (Peters et al., 2000; Peters and Sethares, 2002). Additionally, nerve fiber loss in the anterior commissure has been shown to correlate with indices of global cognitive impairment (Sandell and Peters, 2003).

Analysis of the associations of myelinated nerve fiber deterioration in the genu and cingulate bundle with behavior suggests that both nerve fiber loss and damage to myelin sheaths influences cognitive performance in a tract specific manner. Despite ample evidence for the age-related deterioration of myelinated nerve fibers in the genu, there is little indication that the integrity of the corpus callosum is critical for normal cognitive performance. Only, the frequency of degenerating axon profiles correlates with scores on the 2-minute delay phase of the DNMS task, and not with overall cognitive decline. This is not unexpected, in light of studies of the behavioral effects of callosectomy on humans, in which callosectomy is associated with a specific clinical syndrome that is not generally associated with marked impairments in learning or memory (Oepen et al., 1988; Hutter et al., 1997).

Conversely, deterioration of myelinated nerve fibers in the cingulate bundle is highly correlated with age-related impairments in rule learning and short-term memory. In the cingulate bundle, overall cognitive impairment correlates with the percentage of myelinated nerve fiber profiles having degenerating axons, altered myelin sheaths, dense sheaths, and redundant sheaths. This is not surprising because the cingulate bundle links prefrontal, cingulate, and medial temporal areas (Goldman-Rakic et al., 1984; Morris et al., 1999) that are critical to cognitive processing in general, and memory functions in particular (Goldman Rakic, 1988; Miller and Cohen, 2001). Thus, while the degeneration of nerve fibers with age appears to be a ubiquitous phenomenon, the likelihood that the deterioration of an specific tract effects cognition appears to depend on which cortical areas are connected by that tract.

Conclusions

The present analysis of the integrity of myelinated nerve fibers in the genu of the corpus callosum and cingulate bundle provides further evidence that white matter in the normally aging primate brain deteriorates. With advancing age, myelinated nerve fibers are lost and there is an increased occurrence of myelin sheaths showing degenerative changes. Concurrently, deteriorations of myelin sheaths may be offset to some extent by remyelination. These degenerative and reparative changes appear to be ubiquitous throughout aging subcortical white matter and they contribute to impairments in cognitive function, especially when they involve white matter tracts critical for the processing of information related to learning and memory.

Acknowledgments

The authors wish to thank Ms. Claire Folger for her technical expertise and guidance, as well as the staff of the Laboratory for Cognitive Neurobiology at Boston University School of Medicine, who were invaluable in the collection of behavioral data, and processing of tissue used in this study. This research is supported by NIH grants P01-AG00001 and P51-RR-00165.

Grant Support: National Institutes of Health, National Institute of Aging; Program Project Grant P01-AG000001

Citations

Albert, MS. Cognitive Function. In: Albert, MS.; Moss, MB., editors. Geriatric Neuropsychology. The Guilford Press; New York: 1988. p. 33-53.

Albert MS. Neuropsychological and neurophysiological changes in healthy adult humans across the age range. Neurobiol Aging. 1993; 14:623–625. [PubMed: 8295666]

Allen JS, Bruss J, Brown CK, Damasio H. Normal neuroanatomical variation due to age: the major lobes and a parcellation of the temporal region. Neurobiol Aging. 2005; 26:1245–1260. discussion 1279-1282. [PubMed: 16046030]

Barbas H, Pandya DN. Topography of commissural fibers of the prefrontal cortex in the rhesus monkey. Exp Brain Res. 1984; 55:187–191. [PubMed: 6745350]

Blakemore WF. Observations on oligodendrocyte degeneration, the resolution of status spongiosus and remyelination in cuprizone intoxication in mice. J Neurocytol. 1972; 1:413–426. [PubMed: 8530973]

Blakemore WF, Palmer AC, Noel PR. Ultrastructural changes in isoniazid-induced brain oedema in the dog. J Neurocytol. 1972; 1:263–278. [PubMed: 8530965]

Blakemore WF, Welsh CJ, Tonks P, Nash AA. Observations on demyelinating lesions induced by Theiler's virus in CBA mice. Acta Neuropathol (Berl). 1988; 76:581–589. [PubMed: 3201921]

Cerghet M, Skoff RP, Bessert D, Zhang Z, Mullins C, Ghandour MS. Proliferation and death of oligodendrocytes and myelin proteins are differentially regulated in male and female rodents. J Neurosci. 2006; 26:1439–1447. [PubMed: 16452667]

Cullen MJ, Webster HD. Remodeling of optic nerve myelin sheaths and axons during metamorphosis in Xenopus laevis. J Comp Neurol. 1979; 184:353–362. [PubMed: 762287]

Feldman ML, Peters A. Ballooning of myelin sheaths in normally aged macaques. J Neurocytol. 1998; 27:605–614. [PubMed: 10405027]

Gazzaley AH, Thakker MM, Hof PR, Morrison JH. Preserved number of entorhinal cortex layer II neurons in aged macaque monkeys. Neurobiol Aging. 1997; 18:549–553. [PubMed: 9390783]

Gittins R, Harrison PJ. Neuronal density, size and shape in the human anterior cingulate cortex: a comparison of Nissl and NeuN staining. Brain Res Bull. 2004; 63:155–160. [PubMed: 15130705]

Gledhill RF, McDonald WI. Morphological characteristics of central demyelination and remyelination: a single-fiber study. Ann Neurol. 1977; 1:552–560. [PubMed: 883767]

Goldman-Rakic PS, Selemon LD, Schwartz ML. Dual pathways connecting the dorsolateral prefrontal cortex with the hippocampal formation and para-hippocampal cortex in the rhesus monkey. Neuroscience. 1984; 12:719–743. [PubMed: 6472617]

Goldman-Rakic PS. Topography of cognition: parallel distributed networks in primate association cortex. Annu Rev Neurosci. 1988; 11:137–156. [PubMed: 3284439]

Gundersen HJG. Notes on the Estimation of the Numerical Density of Arbitrary Particles: the Edge Effect. Journal of Microscopy. 1977; 111:219–223.

Guttmann CR, Jolesz FA, Kikinis R, Killiany RJ, Moss MB, Sandor T, Albert MS. White matter changes with normal aging. Neurology. 1998; 50:972–978. [PubMed: 9566381]

Harding AJ, Halliday GM, Kril JJ. Variation in hippocampal neuron number with age and brain volume. Cereb Cortex. 1998; 8:710–718. [PubMed: 9863698]

Head D, Buckner RL, Shimony JS, Williams LE, Akbudak E, Conturo TE, McAvoy M, Morris JC, Snyder AZ. Differential vulnerability of anterior white matter in nondemented aging with minimal acceleration in dementia of the Alzheimer type: Evidence from diffusion tensor imaging. Cereb Cortex. 2004; 14(4):410–423. [PubMed: 15028645]

Herndon JG, Moss MB, Rosene DL, Killiany RJ. Patterns of cognitive decline in aged rhesus monkeys. Behav Brain Res. 1997; 87:25–34. [PubMed: 9331471]

Hinks GL, Franklin RJ. Delayed changes in growth factor gene expression during slow remyelination in the CNS of aged rats. Mol Cell Neurosci. 2000; 16:542–556. [PubMed: 11083917]

Hirano A. Review of the morphological aspects of remyelination. Dev Neurosci. 1989; 11:112–117. [PubMed: 2663419]

Hutter BO, Spetzger U, Bertalanffy H, Gilsbach JM. Cognition and quality of life in patients after transcallosal microsurgery for midline tumors. J Neurosurg Sci. 1997; 41:123–129. [PubMed: 9273870]

Institute of Laboratory Animal Resources Commission on Life Sciences NRC. Guide For the Care and Use of Laboratory Animals. National Academy Press; Washington D.C.: 1996.

Irvine KA, Blakemore WF. Age increases axon loss associated with primary demyelination in cuprizone-induced demyelination in C57BL/6 mice. J Neuroimmunol. 2006; 175:1–2. 69–76.

Lamar M, Resnick SM. Aging and prefrontal functions: dissociating orbitofrontal and dorsolateral abilities. Neurobiol Aging. 2004; 25:553–558. [PubMed: 15013577]

Lampert PW. A comparative electron microscopic study of reactive, degenerating, regenerating, and dystrophic axons. J Neuropathol Exp Neurol. 1967; 26:345–368. [PubMed: 5229871]

Li WW, Penderis J, Zhao C, Schumacher M, Franklin RJ. Females remyelinate more efficiently than males following demyelination in the aged but not young adult CNS. Exp Neurol. 2006; 202:250–254. [PubMed: 16797535]

Ludwin SK. Central nervous system demyelination and remyelination in the mouse: an ultrastructural study of cuprizone toxicity. Lab Invest. 1978; 39:597–612. [PubMed: 739762]

Ludwin SK. Pathology of demyelination and remyelination. Adv Neurol. 1981; 31:123–168. [PubMed: 7325040]

Makris N, Papadimitriou GM, van der Kouwe A, Kennedy DN, Hodge SM, Dale AM, Benner T, Wald LL, Wu O, Tuch DS, Caviness VS, Moore TL, Killiany RJ, Moss MB, Rosene DL. Frontal connections and cognitive changes in normal aging rhesus monkeys: A DTI study. Neurobiol Aging. 2007; 28(10):1556–67. [PubMed: 16962214]

Marner L, Pakkenberg B. Total length of nerve fibers in prefrontal and global white matter of chronic schizophrenics. J Psychiatr Res. 2003; 37:539–547. [PubMed: 14563386]

Mason JL, Langaman C, Morell P, Suzuki K, Matsushima GK. Episodic demyelination and subsequent remyelination within the murine central nervous system: changes in axonal calibre. Neuropathol Appl Neurobiol. 2001; 27:50–58. [PubMed: 11299002]

Meier-Ruge W, Ulrich J, Bruhlmann M, Meier E. Age-related white matter atrophy in the human brain. Ann N Y Acad Sci. 1992; 673:260–269. [PubMed: 1485724]

Merrill DA, Chiba AA, Tuszynski MH. Conservation of neuronal number and size in the entorhinal cortex of behaviorally characterized aged rats. J Comp Neurol. 2001; 438:445–456. [PubMed: 11559900]

Miller EK, Cohen JD. An integrative theory of prefrontal cortex function. Annu Rev Neurosci. 2001; 24:167–202. [PubMed: 11283309]

Moore TL, Killiany RJ, Herndon JG, Rosene DL, Moss MB. Impairment in abstraction and set shifting in aged rhesus monkeys. Neurobiol Aging. 2003; 24:125–134. [PubMed: 12493558]

Moore TL, Killiany RJ, Herndon JG, Rosene DL, Moss MB. Executive system dysfunction occurs as early as middle age in the rhesus monkey. Neurobiol Aging. 2006; 27:1484–1493. [PubMed: 16183172]

Morris R, Pandya DN, Petrides M. Fiber system linking the mid-dorsolateral frontal cortex with the retrosplenial/presubicular region in the rhesus monkey. J Comp Neurol. 1999; 407:183–192. [PubMed: 10213090]

Morrison JH, Hof PR. Life and death of neurons in the aging brain. Science. 1997; 278:412–419. [PubMed: 9334292]

Moss MB, Killiany RJ, Lai ZC, Rosene DL, Herndon JG. Recognition memory span in rhesus monkeys of advanced age. Neurobiol Aging. 1997; 18:13–19. [PubMed: 8983028]

Moss MB, Rosene DL, Peters A. Effects of aging on visual recognition memory in the rhesus monkey. Neurobiol Aging. 1988; 9:495–502. [PubMed: 3062461]

Mufson EJ, Pandya DN. Some observations on the course and composition of the cingulum bundle in the rhesus monkey. J Comp Neurol. 1984; 225:31–43. [PubMed: 6725639]

Nielsen K, Peters A. The effects of aging on the frequency of nerve fibers in rhesus monkey striate cortex. Neurobiol Aging. 2000; 21:621–628. [PubMed: 11016530]

Oepen G, Schulz-Weiling R, Zimmermann P, Birg W, Straesser S, Gilsbach J. Neuropsychological assessment of the transcallosal approach. Eur Arch Psychiatry Neurol Sci. 1988; 237:365–375. [PubMed: 3181223]

O'Sullivan M, Jones DK, Summers PE, Morris RG, Williams SC, Markus HS. Evidence for cortical "disconnection" as a mechanism of age-related cognitive decline. Neurology. 2001; 57:632–638. [PubMed: 11524471]

Pakkenberg B, Gundersen HJ. Neocortical neuron number in humans: effect of sex and age. J Comp Neurol. 1997; 384:312–320. [PubMed: 9215725]

Pandya, DN.; Rosene, DL. Some observations on trajectories and topography of commissural fibers. In: Reeves, AG., editor. Epilepsy and the Corpus Callosum. Plenum Press; New York: 1985. p. 21-39.

Peters A, Leahu D, Moss MB, McNally KJ. The effects of aging on area 46 of the frontal cortex of the rhesus monkey. Cereb Cortex. 1994; 4:621–635. [PubMed: 7703688]

Peters A, Morrison JH, Rosene DL, Hyman BT. Feature article: are neurons lost from the primate cerebral cortex during normal aging? Cereb Cortex. 1998; 8:295–300. [PubMed: 9651126]

Peters A, Moss MB, Sethares C. Effects of aging on myelinated nerve fibers in monkey primary visual cortex. J Comp Neurol. 2000; 419:364–376. [PubMed: 10723011]

Peters, A.; Palay, SL.; Webster, DH. The Fine Structure of the Nervous System: Neurons and their Supporting Cells. Oxford University Press; New York: 1991.

Peters A, Rosene DL. In aging, is it gray or white? J Comp Neurol. 2003; 462:139–143. [PubMed: 12794738]

Peters A, Sethares C. Aging and the myelinated fibers in prefrontal cortex and corpus callosum of the monkey. J Comp Neurol. 2002; 442:277–291. [PubMed: 11774342]

Peters A, Sethares C. Is there remyelination during aging of the primate central nervous system? J Comp Neurol. 2003; 460:238–254. [PubMed: 12687688]

Peters A, Sethares C, Killiany RJ. Effects of age on the thickness of myelin sheaths in monkey primary visual cortex. J Comp Neurol. 2001; 435:241–248. [PubMed: 11391644]

Powell HC, Lampert PW. Oligodendrocytes and their myelin-plasma membrane connections in JHM mouse hepatitis virus encephalomyelitis. Lab Invest. 1975; 33:440–445. [PubMed: 171479]

Presty SK, Bachevalier J, Walker LC, Struble RG, Price DL, Mishkin M, Cork LC. Age differences in recognition memory of the rhesus monkey (Macaca mulatta). Neurobiol Aging. 1987; 8:435–440. [PubMed: 3683724]

Raine CS, Wisniewski H, Prineas J. An ultrastructural study of experimental demyelination and remyelination. II. Chronic experimental allergic encephalomyelitis in the peripheral nervous system. Lab Invest. 1969; 21:316–327. [PubMed: 5343503]

Rapp PR, Amaral DG. Evidence for task-dependent memory dysfunction in the aged monkey. J Neurosci. 1989; 9:3568–3576. [PubMed: 2795141]

Rosenbluth J. Redundant myelin sheaths and other ultrastructural features of the toad cerebellum. J Cell Biol. 1966; 28:73–93. [PubMed: 5901501]

Rosenbluth, J. Glial Membranes and Axoglial Junctions. In: Waxman, SG.; Koscis, JD.; Stys, PK., editors. The axon: structure, function, and pathophysiology. Oxford University Press; New York: 1995. p. 613-633.

Salat DH, Tuch DS, Greve DN, van der Kouwe AJ, Hevelone ND, Zaleta AK, Rosen BR, Fischl B, Corkin S, Rosas HD, Dale AM. Age-related alterations in white matter microstructure measured by diffusion tensor imaging. Neurobiol Aging. 2005; 26:1215–1227. [PubMed: 15917106]

Sandell JH, Peters A. Effects of age on nerve fibers in the rhesus monkey optic nerve. J Comp Neurol. 2001; 429:541–553. [PubMed: 11135234]

Sandell JH, Peters A. Disrupted myelin and axon loss in the anterior commissure of the aged rhesus monkey. J Comp Neurol. 2003; 466:14–30. [PubMed: 14515238]

Schmahmann, JD.; Pandya, DN. Fiber pathways of the brain. Oxford University Press, Inc.; New York: 2006.

Shen S, Sandoval J, Swiss VA, Li J, Dupree J, Franklin RJ, Casaccia-Bonnefil P. Age-dependent epigenetic control of differentiation inhibitors is critical for remyelination efficiency. Nat Neurosci. 2008; 11:1024–1034. [PubMed: 19160500]

Sim FJ, Zhao C, Penderis J, Franklin RJ. The age-related decrease in CNS remyelination efficiency is attributable to an impairment of both oligodendrocyte progenitor recruitment and differentiation. J Neurosci. 2002; 22:2451–2459. [PubMed: 11923409]

Smith DE, Rapp PR, McKay HM, Roberts JA, Tuszynski MH. Memory impairment in aged primates is associated with focal death of cortical neurons and atrophy of subcortical neurons. J Neurosci. 2004; 24:4373–4381. [PubMed: 15128851]

Sturrock RR. Changes in neuroglia and myelination in the white matter of aging mice. J Gerontol. 1976; 31:513–522. [PubMed: 950445]

Sullivan EV, Adalsteinsson E, Pfefferbaum A. Selective age-related degradation of anterior callosal fiber bundles quantified in vivo with fiber tracking. Cereb Cortex. 2006; 16:1030–1039. [PubMed: 16207932]

Terry RD, DeTeresa R, Hansen LA. Neocortical cell counts in normal human adult aging. Ann Neurol. 1987; 21:530–539. [PubMed: 3606042]

Wisco JJ, Killiany RJ, Guttmann CRG, Warfield SK, Moss MB, Rosene DL. Age-related changes in forebrain white and gray matter volume in aging monkeys: An MRI study using template driven segmentation. Neurobiol Aging. 2008; 29(10):1563–75. [PubMed: 17459528]

Wisniewski H, Raine CS. An ultrastructural study of experimental demyelination and remyelination. V. Central and peripheral nervous system lesions caused by diphtheria toxin. Lab Invest. 1971; 25:73–80. [PubMed: 5555698]

Witelson SF. Hand and sex differences in the isthmus and genu of the human corpus callosum. A postmortem morphological study. Brain. 1989; 112(Pt 3):799–835. [PubMed: 2731030]

Yoon B, Shim YS, Lee KS, Shon YM, Yang DW. Region-specific changes of cerebral white matter during normal aging: A diffusion-tensor analysis. Archiv Gerontol Geriatr. 2008; 47(1):129–38.

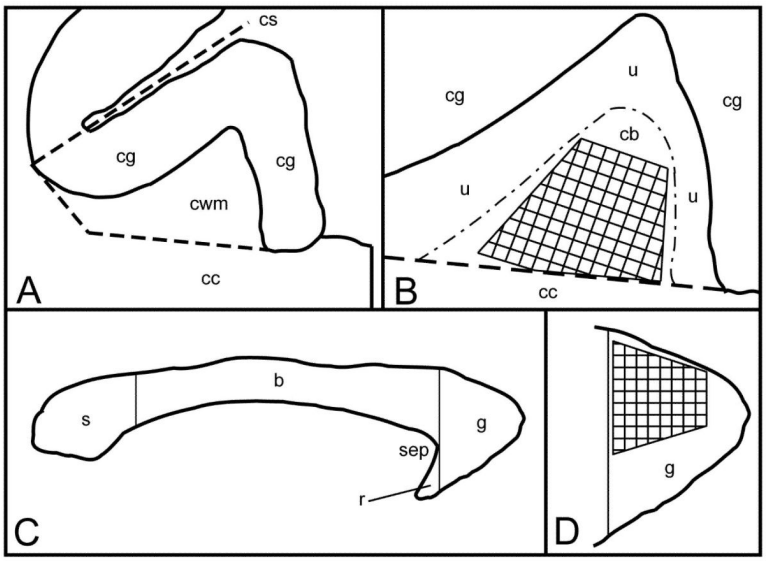

Figure 1.

This figure depicts the cross-sectional areas for the cingulate white matter (A and B) in the coronal plane, and the genu of the corpus callosum (C and D) in the mid-sagittal plane. **A:** The cingulate gyrus and underlying white matter at the level of the anterior commissure. The cingulate white matter (cwm) is bounded dorsally, medially, and laterally by the cingulate cortex (cg). Ventrally, it is bounded by the body of the corpus callosum (cc). An inferolateral boundary was arbitrarily defined by a line oriented perpendicular to the cingulate sulcus (cs), from the gray matter/white matter boundary dorsally, to the underlying corpus callosum (cc) ventrally. **B:** Enlarged diagram of the cingulate white matter from **A**. The cingulate white matter is composed of both the cingulate bundle proper (cb) and local system fibers (u) underlying the cingulate cortex (cg). The hatched area represents the portion of the cingulate bundle sampled for electron microscopic analysis. **C:** A mid-sagittal diagram of the corpus callosum of the rhesus monkey. The genu (g) is the anterior-most portion of the corpus callosum. Its posterior boundary is defined by a straight line, perpendicular to the long axis of the corpus callosum, at the boundary of the corpus callosum with the anterior tip of the septum pellucidum (sep). Splenium (s), body of the corpus callosum (b), rostrum (r). **D:** An enlarged diagram of the mid-sagittal area of genu of the corpus callosum in **C**. The hatched area represents the dorsal portion of the genu sampled for electron microscopic analysis.

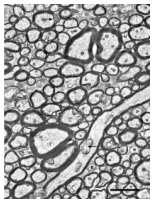

Figure 2.
Electron micrograph of the cingulate bundle of a 9-year-old female rhesus monkey (AM096), showing the tightly packed myelinated nerve fibers. The myelin sheaths of some nerve fibers show shearing defects (arrows), an artifact of tissue processing. Interspersed amongst these myelinated nerve fibers, either singly or in clusters, are unmyelinated nerve fibers (U), as well as nodal (N) and paranodal profiles (P) of myelinated nerve fibers. Scale bar = 2μm.

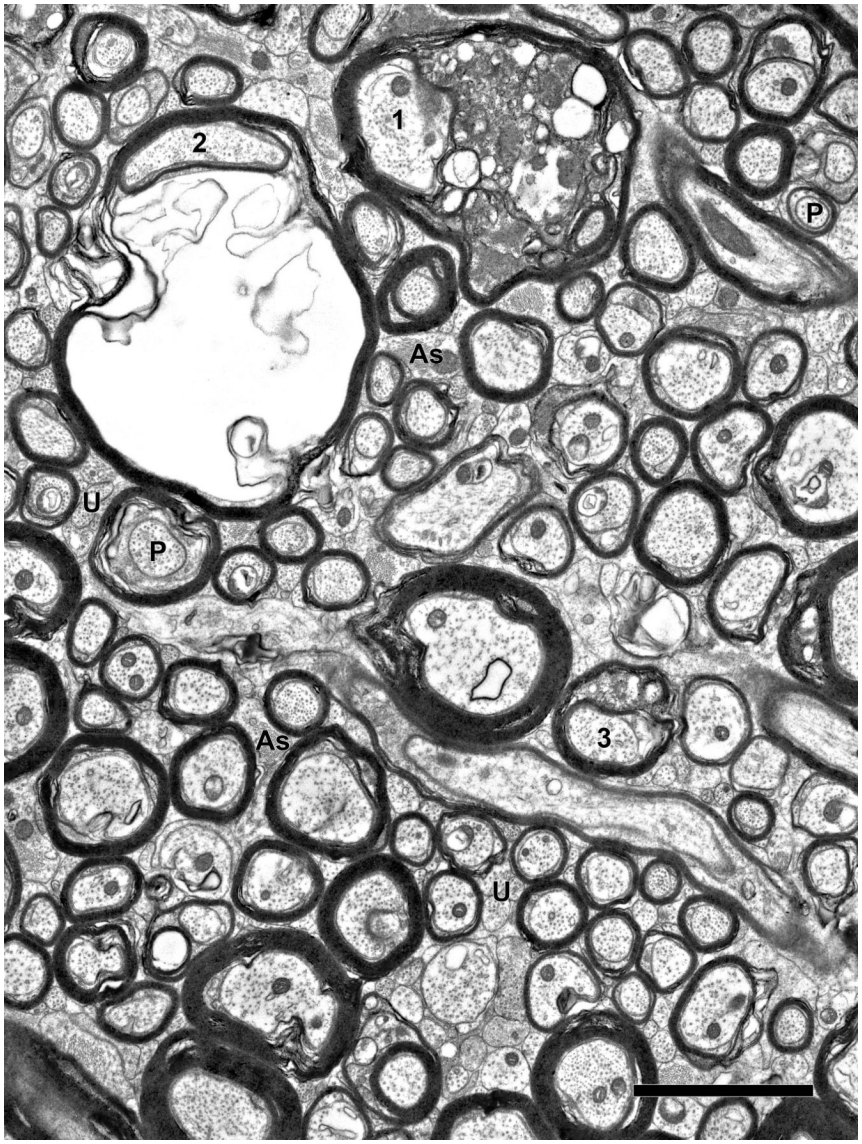

Figure 3.
Electron micrograph of the cingulate bundle of a 24-year-old female rhesus monkey (AM100). The myelinated nerve fibers are less tightly packed than in younger monkeys (Fig. 2), and astrocytic processes (As) are more frequent between adjacent nerve fibers. Some nerve fibers (1 and 3) contain dense cytoplasm in splits of their myelin sheaths. Another myelinated nerve fiber (2) shows ballooning of the sheath. Interspersed amongst these myelinated nerve fibers are unmyelinated nerve fibers (U). Profiles through paranodes (P) are also indicated. Scale bar = 2μm.

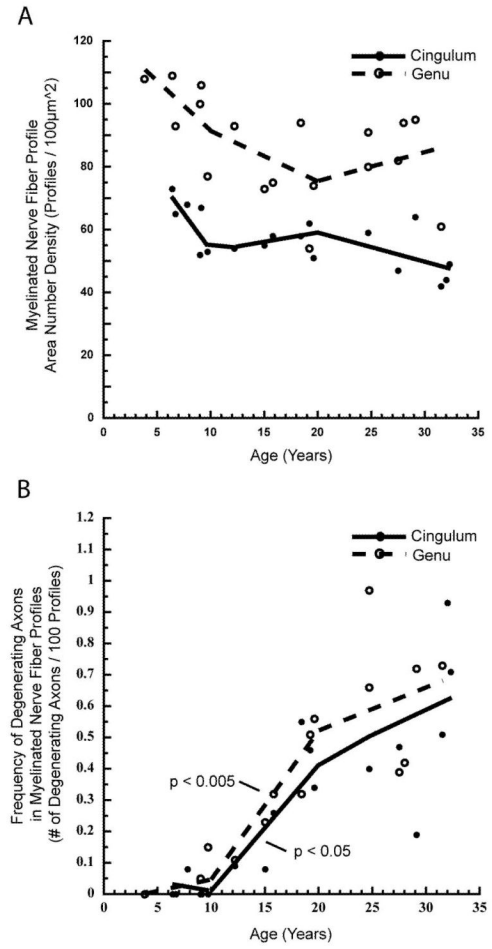

Figure 4.

Scatterplots with piecewise, linear fits showing: **A**) The number of myelinated nerve fibers per unit area, and **B**) the frequency of myelinated nerve fiber profiles with degenerating axons in the cingulate bundle and genu of the corpus callosum of young (<10 years), middle aged (10-20 years), and old (>20 years) rhesus monkeys. In both structures, a decrease in myelinated nerve fibers occurs gradually with age, with none of the three age groups exhibiting a significant change in area number density (**A**). The frequency of degenerating myelinated axons significantly increases only during middle age in both the genu ($p < 0.005$) and cingulate bundle ($p < 0.05$; **B**).

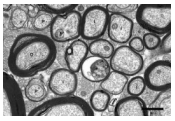

Figure 5.
Electron micrograph from the cingulate bundle of a 31 year-old male rhesus monkey (AM091). Internodal (I) and paranodal (P) profiles of myelinated nerve fibers are indicated. The axon of one myelinated nerve fiber (asterisk) is degenerating. Another myelinated nerve fiber (D) is surrounded by sheath containing dense cytoplasm. Scale bar= 1μm.

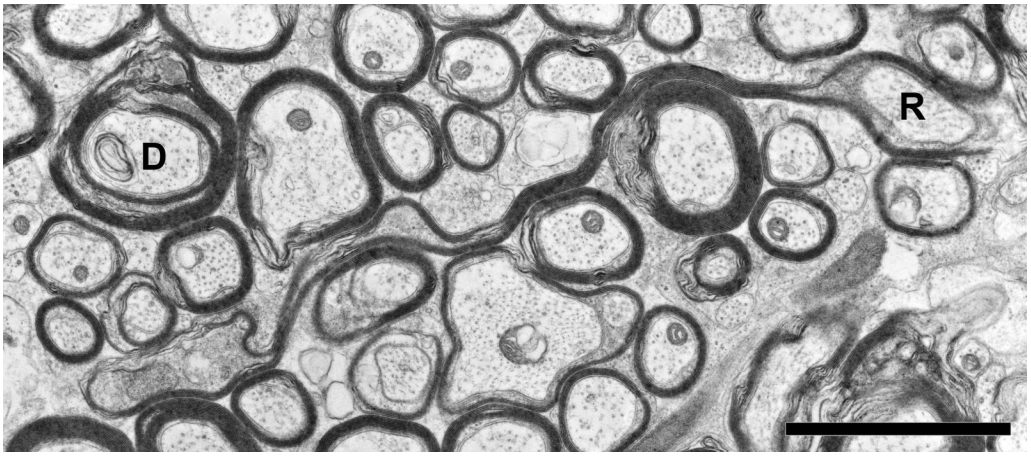

Figure 6.
Electron micrograph of the cingulate bundle of an 18.4 year-old female rhesus monkey (AM 221). One axon (R), is ensheathed by a myelin sheath too large for the axon, referred to as a redundant sheath, while a second axon (D) is enclosed by a sheath with a split at the major dense line, referred to as a dense sheath Scale bar = 2μm.

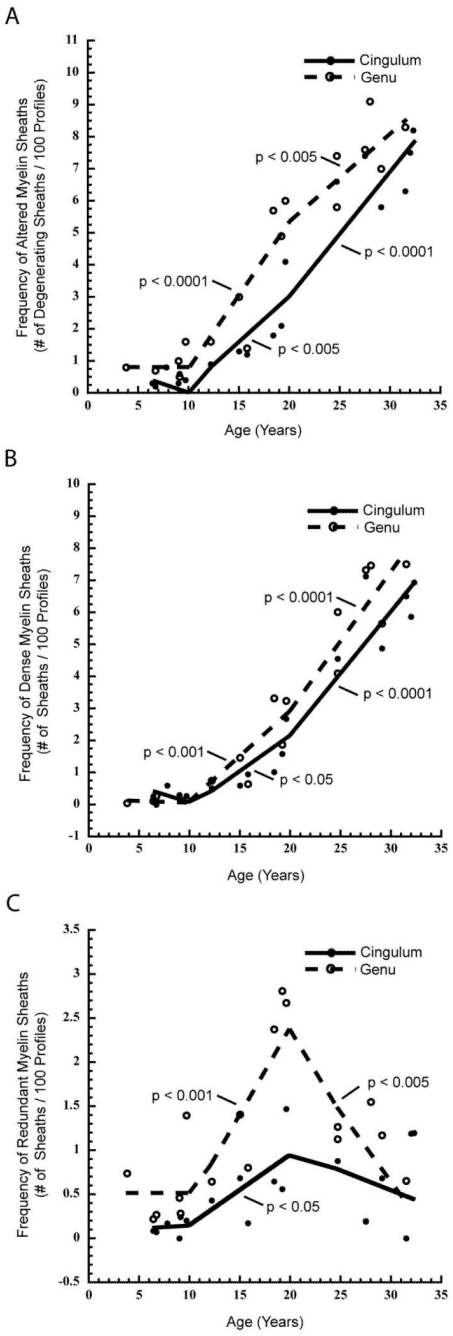

Figure 7.

Scatterplots with a piecewise, linear fits showing: **A**) the frequency of myelinated nerve fiber profiles with altered myelin sheaths (including dense sheaths, redundant sheaths, and myelin balloons), **B**) the frequency of myelinated nerve fiber profiles with dense myelin sheaths, and **C**) the frequency of myelinated nerve fiber profiles with redundant myelin sheaths in the cingulate bundle and the genu of the corpus callosum of young (<10 years), middle aged (10-20 years), and old (>20 years) rhesus monkeys. As shown in **A**, a significant increase in the frequency of total altered myelin sheaths is seen in middle and old age groups in both the genu (middle age, $p < 0.0001$; old, $p < 0.005$) and cingulate bundle (middle age, $p < 0.005$; old, $p < 0.0001$). Likewise, in **B**, a significant increase in the

frequency of dense myelin sheaths is seen in middle and old age groups in both the genu (middle age, $p < 0.001$; old, $p < 0.0001$) and cingulate bundle (middle age, $p < 0.05$; old, $p < 0.0001$). In **C**, a significant increase in the frequency of redundant myelin sheaths is evident in middle age monkeys in both the genu ($p < 0.001$) and cingulate bundle ($p < 0.05$). Additionally, there is a significant decrease in the frequency of redundant myelin sheaths in the genu of old aged monkeys ($p < 0.005$) but not in the cingulate bundle.

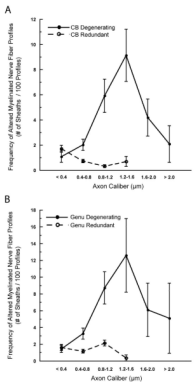

Figure 8.

Line graphs showing the frequency of degenerating (dense sheaths and balloons) and of redundant myelin sheaths in the cingulate bundle (**A**) and genu of the corpus callosum (**B**) as a function of mean axon diameter in monkeys over 10 years of age. Nerve fibers are divided into 6 size classes from < 0.4μm to > 2.0μm in diameter.

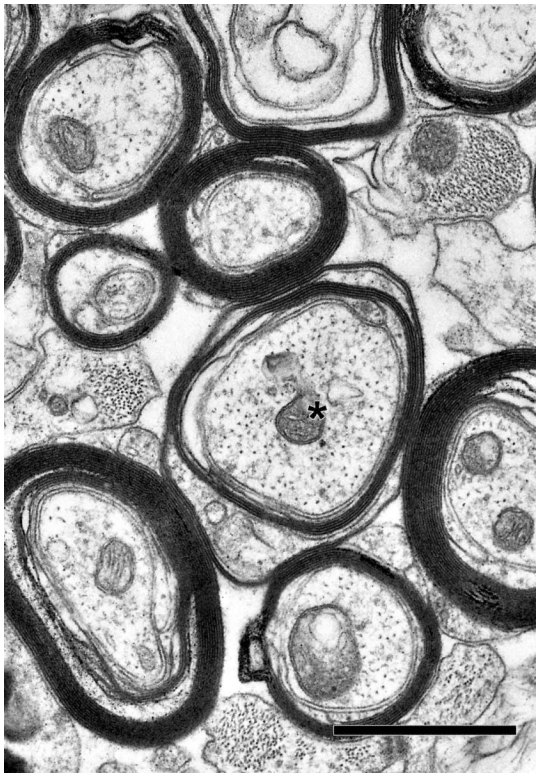

Figure 9.
Electron micrograph of the cingulate bundle of a 31-year-old male rhesus monkey (AM091). The indicated axon (asterisk) is thinly myelinated. Scale bar = 1μm

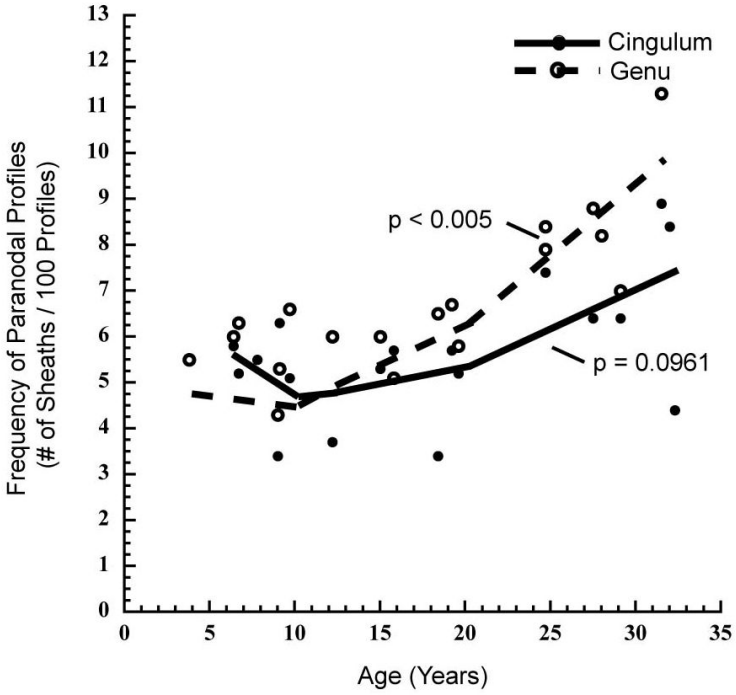

Figure 10.

Scatterplot with a piecewise, linear fit showing the frequency of myelinated nerve fiber profiles through paranodes in the cingulate bundle and genu of the corpus callosum of young (<10 years), middle aged (10-20 years), and old (>20 years) monkeys. A change in the frequency of paranodal profiles is most prominent in old age, significantly increasing in the genu of the corpus callosum ($p < 0.005$), and exhibiting a trend toward a significant increase in the cingulate bundle ($p = 0.0961$) of old monkeys. No significant age-group specific changes in paranodal frequency are evident in either structure in young or middle aged monkeys.

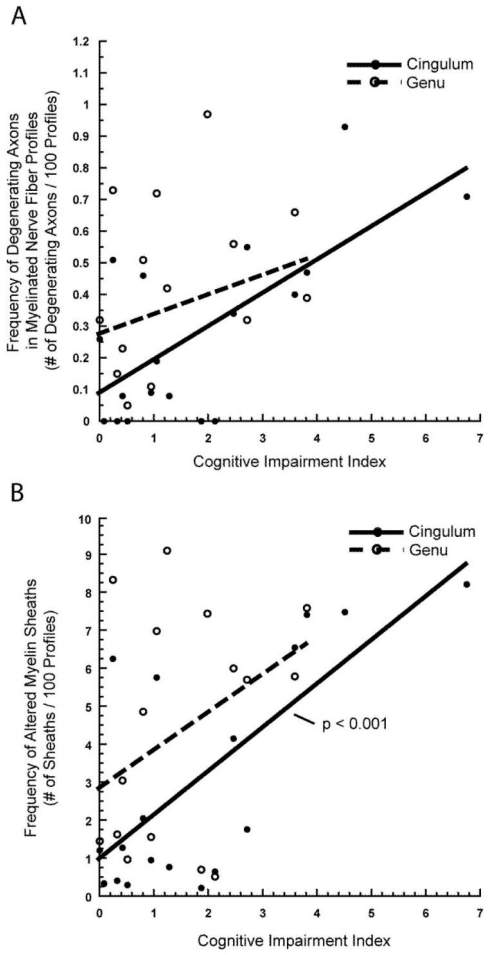

Figure 11.

A) Scatterplot with a linear fit, showing the frequency of myelinated nerve fiber profiles with degenerating axons in the cingulate bundle and genu of the corpus callosum versus a measure of global cognitive impairment, the cognitive impairment index (CII). An increase in CII, indicating worsening cognitive function, is associated with an increase in the frequency of degenerating axons in the cingulate bundle ($p < 0.005$) but not in the genu of the corpus callosum ($p = 0.2465$). **B**) Scatterplot with a linear fit, showing the frequency of myelinated nerve fiber profiles with altered myelin sheaths in the cingulate bundle and genu of the corpus callosum versus CII. Worsening cognitive function is significantly associated with an increased frequency of altered myelin sheaths in the cingulate bundle ($p < 0.001$) but not the genu ($p = 0.1086$).

Table 1

Performance on Tasks of Rule Learning and Memory

This table summarizes the performance of 21 rhesus monkeys on five tests of recognition memory: the acquisition and two delay phases of the Delayed Non-Match to Sample (DNMS) task, and object and spatial versions of the Delayed Recognition Span Task (DRST). Each individual monkey's performance was normalized to 53 adult monkeys to generate a score of global cognitive impairment, which is presented here as the cognitive impairment index (CII).

			DNMS			DRST		CII
Subject	**Age**	**Sex**	**Acquisition Errors**	**2 Min. Delay % Correct**	**10 Min. Delay % Correct**	**Spatial Span**	**Object Span**	
AM 058	3.8	M	-	-	-	-	-	-
AM 076	6.4	F	58	91%	74%	2.35	5.28	0.08
AM 129	6.7	F	114	75%	71%	2.24	2.47	1.87
AM 130	7.8	F	121	84%	72%	2.32	2.92	1.28
AM 047	9.0	M	21	95%	87%	2.23	3.58	0.51
AM 096	9.1	F	181	84%	65%	2.11	3.00	2.12
AM 053	9.7	M	71	93%	82%	2.06	3.39	0.32
AM 042	12.2	M	40	83%	-	-	-	0.95
AM 144	15.0	M	42	88%	78%	1.94	2.73	0.42
AM 143*	15.8	M	36	86%	84%	2.56	4.46	0.00
AM 221	18.4	F	200	73%	60%	2.57	3.77	2.71
AM 209	19.2	M	52	79%	76%	2.50	3.90	0.80
AM 133	19.6	M	189	82%	73%	1.96	3.62	2.46
AM 100	24.7	F	241	73%	71%	2.04	2.96	3.59
AM 019	24.7	F	111	72%	-	2.31	-	1.98
AM 062	27.5	M	353	90%	-	2.01	-	3.81
AM 027	28.0	M	101	84%	-	2.08	-	1.24
AM 026	29.1	F	83	85%	-	1.98	-	1.05
AM 091	31.5	M	70	-	-	2.59	3.03	0.25
AM 041	32.0	F	341	74%	-	2.22	-	4.51
AM 023*	32.3	F	481	70%	66%	1.72	1.97	6.75

*Exact age unknown

Table 2

Percentage of Myelinated Nerve Fiber Sheath Changes and Area Number Density

This table gives individual values for cross-sectional area, myelinated nerve fiber density and age-related changes in myelin sheath morphology in the cingulate bundle and genu of the corpus callosum for 21 rhesus monkeys ranging in age from 4 to 32 years of age.

Subject	Age	Sex	Hemispher	Cross-Sectional Area (mm^2)		Myelinated: Nerve Fiber Profiles per 100μm2		% Abnormal Axons		% Altered Myelin Sheaths		% Paranodes	
				Genu	Cingulum	Genu	Cingulum	Genu	Cingulum	Genu	Cingulum	Genu	Cingulum
AM 058	3.8	M	Right	-	-	108	-	0.0	-	0.8	-	5.5	-
AM 076	6.4	F	Left	-	3.5	109	73	0.0	0.0	0.3	0.3	6.0	5.8
AM 129	6.7	F	Left	22.2	4.7	93	65	0.0	0.0	0.7	0.2	6.3	5.2
AM 130	7.8	F	Left	-	2.6	-	68	-	0.1	-	0.8	-	5.5
AM 047	9.0	M	Left	-	4.4	100	52	0.0	0.0	1.0	0.3	4.3	3.4
AM 096	9.1	F	Right	22.9	3.0	106	67	0.0	0.0	0.5	0.6	5.3	6.3
AM 053	9.7	M	Left	16.9	4.1	77	53	0.2	0.0	1.6	0.4	6.6	5.1
Mean	**7.5**			**20.7**	**3.7**	**99**	**63**	**0.0**	**0.0**	**0.8**	**0.4**	**5.7**	**5.2**
Std. Deviation	**1.9**			**3.3**	**0.8**	**12**	**8**	# **0.1**	**0.0**	# **0.5**	**0.2**	# **0.8**	**1.0**
AM 042	12.2	M	Left	15.2	5.7	93	54	0.1	0.1	1.6	0.9	6.0	3.7
AM 144	15.0	M	Right	20.9	4.2	73	55	0.2	0.1	3.0	1.3	6.0	5.3
AM 143*	15.8	M	Left	19.5	5.2	75	58	0.3	0.3	1.4	1.2	5.1	5.7
AM 221	18.4	F	Right	-	2.9	94	58	0.3	0.5	5.7	1.8	6.5	3.4
AM 209	19.2	M	Right	-	4.3	54	62	0.5	0.5	4.9	2.1	6.7	5.7
AM 133	19.6	M	Left	18.3	4.6	74	51	0.6	0.3	6.0	4.1	5.8	5.2
Mean	**16.7**			**18.5**	**4.5**	**77**	**56**	**0.3**	**0.3**	**3.8**	**1.9**	**6.0**	**4.8**
Std. Deviation	**2.6**			**2.4**	**1.0**	**15**	**4**	# **0.2**	**0.2**	# **2.0**	**1.2**	# **0.6**	**1.0**
AM 100	24.7	F	Left	5.8	3.6	91	59	0.7	0.4	5.8	6.6	7.9	7.4
AM 019	24.7	F	Left	9.9	-	80	-	1.0	-	7.4	-	8.4	-
AM 062	27.5	M	Right	-	2.7	82	47	0.4	0.5	7.6	7.4	8.8	6.4
AM 027	27.97	M	Right	-	-	94	-	0.4	-	9.1	-	8.2	-
AM 026	29.1	F	Left	-	3.7	95	64	0.7	0.2	7.0	5.8	7.0	6.4
AM 091	31.5	M	Left	-	3.4	61	42	0.7	0.5	8.3	6.3	11.3	8.9
AM 041	32.0	F	Right	-	4.1	-	44	-	0.9	-	7.5	-	8.4
AM 023*	32.3	F	Left	-	5.6	-	49	-	0.7	-	8.2	-	4.4

Subject	Age	Sex	Hemispher	Cross-Sectional Area (mm^2)		Myelinated: Nerve Fiber Profiles per 100μm2		% Abnormal Axons		% Altered Myelin Sheaths		% Paranodes	
				Genu	Cingulum	Genu	Cingulum	Genu	Cingulum	Genu	Cingulum	Genu	Cingulum
Mean	**29.3**			**7.9**	**3.9**	**84**	**49**	**0.6**	**0.6**	**7.9**	**7.0**	**8.7**	**6.9**
Std. Deviation	**2.6**			**2.9**	**1.1**	**13**	**9** #	**0.2**	**0.3** #	**0.8**	**1.0** #	**1.6**	**1.8**

*Exact age unknown